Brain Struct Funct (2010) 215:105–113
DOI 10.1007/s00429-010-0275-8

ORIGINAL ARTICLE

Targeting of neural stem cells in the hippocampus of adult rats by custom-made Ad vectors

Steve Hildebrandt · Anke Schmidt · Anja Stoll · Oliver Schmitt · Rüdiger Köhling · Andreas Wree · Stefan J.-P. Haas · Brigitte M. Pützer

Received: 15 April 2010 / Accepted: 5 July 2010 / Published online: 22 July 2010

Abstract Adult hippocampal neural stem cells (NSC) are an intriguing source for cell replacement or could serve as delivery vehicles for therapeutic genes. We recently reported selective transduction of adult mouse NSC in the DG by in vivo injection of GFP encoding adenoviral (Ad) vectors engineered to bind NSC-specific peptides. Here, we investigated the specificity of these peptide-tagged vectors in the adult rat DG, and whether they can be used to follow differentiation of infected cells over time. The virus-containing solution was injected into the DG by stereotaxic surgery. Specific transduction of NSC was demonstrated by the radial glia-like morphology of GFP-expressing type-1 cells and co-labeling with nestin or glial fibrillary acidic protein. Three days post-injection more than 82% of GFP-containing cells were nestin-immunoreactive, as revealed by unbiased stereology and no GFP-expressing neurons were observed. However, 30 days after injection, the amount of GFP and nestin-containing cells declined (56%), whereas now neurons that contained NeuN or possessed the typical granular nerve cell morphology expressed GFP, indicating that they were derived from initially transduced NSC. Importantly, still more than 20% of nestin-immunoreactive NSC was found to be GFP-positive 90 days after infection, but unfortunately at this time point no GFP-containing neurons were detectable. Our results demonstrate that Ad vectors tagged with NSC-specific ligands can be used to target type-1 NSC, the low-proliferating cell population, in the rat hippocampus. They are a valuable tool to monitor the differentiation of their descendants, at least over short time periods.

Keywords Adult rat brain · Dentate gyrus · Adenovirus · Stereotaxy · Neuroanatomy · In vivo gene transfer

Introduction

Over a long time, it was thought that new neurons could not be generated in the adult mammalian brain. Meanwhile, it is well accepted that there are two regions in the brain, the dentate gyrus in the hippocampus and the olfactory bulb (from neural stem cells lying far away in the subventricular zone, SVZ), where lifelong neurogenesis occurs. This has been demonstrated mainly in rodents (Kempermann 2006), but has also been shown to be true for humans (Eriksson et al. 1998; Curtis et al. 2003; Ming and Song 2005). It is supposed that there are stem cells in the hippocampus that are able to divide and give rise to a daughter cell that remains in a stem cell state and another daughter cell that can differentiate into a neuron or a glial cell. These neural stem cells (NSC), called type-1 cells, possess a radial glia-like morphology. The soma of these cells is located in the subgranular zone, their single process goes through the granular zone, and they express both the characteristic intermediate filaments nestin and glial fibrillary acidic protein (GFAP) (Kempermann et al. 2004). In contrast to type-1 cells that have a low dividing rate (Kronenberg et al. 2003), their daughter cells (so called

S. Hildebrandt and A. Schmidt contributed equally to this work.

S. Hildebrandt · O. Schmitt · A. Wree · S. J.-P. Haas (✉)
Institute of Anatomy, Medical Faculty, University of Rostock, Gertrudenstr. 9, 18057 Rostock, Germany
e-mail: stefan.haas@uni-rostock.de

A. Schmidt · A. Stoll · B. M. Pützer
Department of Vectorology and Experimental Gene Therapy, Biomedical Research Center, Rostock, Germany

R. Köhling
Institute of Physiology, Medical Faculty, University of Rostock, Rostock, Germany

type-2 cells), which are putative neuronal progenitor cells, divide more rapidly (Kempermann et al. 2004; Steiner et al. 2006).

Many groups are studying the maturation and integration of newly generated neurons (Song et al. 2005). However, for all these studies a major problem is how to label these newly generated neurons. Classical methods to label proliferating cells with thymidine analogs as tritiated thymidine (Altman and Das 1965) or 5-bromo-2′-deoxyuridine (BrdU) (Dolbeare 1995; Kempermann 2006) need histological or immunohistochemical detection methods that could interfere with cell type specific labeling methods in the tissue and moreover, allow only the assignment of marker proteins or structures nearby the nucleus of a newborn neuron. Hence, morphological investigations of axons, synapses or physiological studies are not possible or limited. Moreover, after several cell divisions the content of previously applied thymidine analogs could be below the detection limit (Dolbeare 1995; Kempermann 2006). Another more recent method to label proliferating cells is performed by stereotactic injection of retro- and lentiviruses into the hippocampus (van Praag et al. 2002; Overstreet et al. 2004; Geraerts et al. 2006; Kempermann 2006; Zhao et al. 2006; Ge et al. 2007). Successfully transduced cells, their morphology and processes can be visualized by reporter genes. This method, however, allows labeling primarily cells that are in a mitotic state during virus infection, such as type-2 cells, whereas type-1 cells are not detectable. Transgenic animals that express GFP under the stem/progenitor cell-specific nestin promoter can also not be used for differentiation studies. During maturation, when the amount of stem cell-specific proteins decreases, the GFP-content also decreases (Kronenberg et al. 2003).

We recently published a new method that allows us selective targeting of NSC of adult mice by direct in vivo injection of Ad vectors linked to peptide ligands that specifically bind to hippocampal stem cells (Schmidt et al. 2007). The aim of the present contribution is to investigate their potential to transduce specific stem cells in the adult rat brain, and whether they can be used to follow differentiation of infected cells, respectively their daughter cells, over longer time periods. This is of particular interest to gathering a broader spectrum for vector application in rat animal models of CNS disorders.

Materials and methods

Adenovirus vector production, pegylation of viruses and peptide coupling

Adenoviral wild-type vector expressing GFP (Pützer et al. 2000), and a CAR-ablated AdTLY477RAE vector with GFP-luciferase expression (named AdGFPL) (Alemany and Curiel 2001) have been described previously. All viruses were propagated, purified and titrated by standard methods (Graham and Prevec 1995; Pützer et al. 1997). The peptide VPTQSSG was covalently linked to Ad vectors by a bifunctional crosslinker NHS-PEG_4-maleimide (Thermo Scientific, Germany). Briefly, bifunctional NHS-PEG_4-Mal was added to the virus with 5% w/v. To allow coupling of PEG to the adenovirus surface by reaction of *N*-hydroxysuccinimide with primary amines of viruses at pH 8–9, samples were incubated by stirring for 2 h at 4°C. Repeated CsCl centrifugation was performed to separate unbound PEG from the PEGylated viruses followed by dialysis overnight at 4°C (O'Riordan et al. 1999). The sulfhydryl-containing peptide dissolved in PBS (10 mM) was added to PEGylated virus to react with maleimide groups at a concentration of 1 mM and incubated by stirring for 4 h at 4°C. Separation of unreacted peptides was then achieved by dialysis overnight (Romanczuk et al. 1999).

Intrahippocampal and subventricular zone Ad vector injections

Young adult male Wistar rats about 9 weeks of age ($n = 22$) were obtained from Charles River Laboratories. Rats were housed in a dedicated pathogen-free animal facility under a 12 h light/dark cycle with free access to food and water. Adenoviral vectors were injected into the right dentate gyrus (DG) of the hippocampus ($n = 19$) (Fig. 1a) or into the right SVZ beneath the lateral ventricle ($n = 3$; Fig. 1d). Briefly, rats were anesthetized by intraperitoneal injection of ketamine (75 mg/kg) and rompun (5.8 mg/kg) and mounted in a rat stereotaxic apparatus (Kopf). The skull was opened with a dental thrill and Ad vectors (appr. 10^5–10^6 pfu/brain diluted into 2 µl) were injected into the DG by using a glass capillary with an outer diameter of about 70 µm mounted onto a 5 µl Hamilton syringe. The coordinates with reference to bregma were for the DG: AP: −3.8 mm, L: −1.6 mm, DV: −3.6 mm (dura). For the SVZ injections the following coordinates referring to bregma were used: AP: +1.2 mm, L: −1.3 mm, DV: −4.3 mm (dura) (Paxinos 1986). All animal procedures were conducted in accordance with the german guidelines and with approval of the local authorities.

Immunohistochemistry

As much as 3 days ($n = 7$), 30 days ($n = 6$) or 90 days ($n = 6$) after virus injection, animals were euthanized and brains were prepared for immunohistochemistry as described below. After anesthesia with an overdose of pentobarbital-Na^+ (80 mg/kg), rats were perfused with

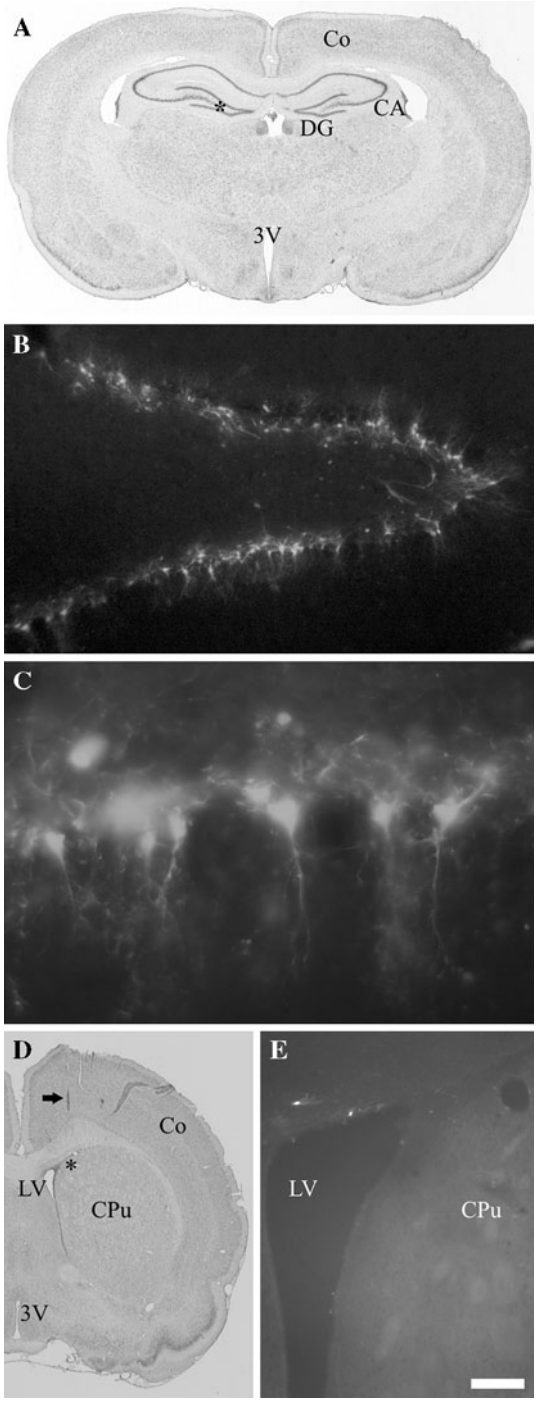

Fig. 1 Location of injection site and GFP-distribution documented by epifluorescence microscopy. **a** Silver Nissl staining of frontal section: the Ad-vector injection site in the hilar region of the DG is marked with an *asterisk*. **b** GFP-expressing cells are restricted to the DG and in higher magnification (**c**) their type-1 cell phenotype is obvious. **d** The injection site for the SVZ is marked in a Nissl stained frontal section (*asterisk*) and the injection tract is labeled with an *arrow*. **e** Only single cells with astroglial morphology expressing GFP were observed. *3V* third ventricle, *CA* cornu ammonis, *DG* dentate gyrus, *Co* cortex, *CPu* caudate putamen (striatum), *LV* lateral ventricle. *Scale bar* **a**, **d** 150 μm, **b**, **e** 100 μm, **c** 25 μm

50 ml isotonic NaCl-solution followed by 400 ml of 3.7% paraformaldehyde (dissolved in 0.1 M PBS, pH 7.4). Brains were immediately removed from the skull, postfixed overnight followed by an incubation overnight in PBS containing 20% sucrose at 4°C, and finally frozen in isopentane (−50°C) and stored at −80°C. Brains were cut in to 30 μm thick serial sections using a cryostat (Leica) and parallel tissue slices were stored in a cryoprotection solution at −20°C until immunohistochemically stained. One series of parallel sections was immediately mounted on glass slides and Nissl or silver Nissl stainings according to Schmitt and Eggers (1997) were performed. Sections were washed three times with PBS, blocked for 1 h at room temperature (PBS with 3% BSA, 3% normal goat serum and 0.05% Triton X-100), and incubated with primary antibodies against nestin for NSC (1:500, ms, Becton–Dickinson) or GFAP for radial glia-like hippocampal type-1 NSC (1:400, rb, Sigma) in combination with antibodies against the neuronal nuclei antigen for post-mitotic neurons (NeuN, 1:500, ms, Chemicon) solved in PBS/1% BSA/0.025% Triton X-100 overnight at 4°C. After washing, the sections were incubated with Cy3-conjugated anti-mouse (1:500, Dianova) and AMCA-conjugated anti-rabbit (1:500, Dianova) secondary antibodies. Brain sections, after rinsing in PBS, were mounted onto SuperFrostPlus glass slides (Menzel, Braunschweig, Germany), air dried and finally covered with a fluorescence mounting medium.

Stereology and documentation of immunohistochemical stainings

We used unbiased respective design-based stereology (West 1993) to evaluate GFP and GFP-nestin double-labeled neural progenitor cells. A computer-assisted microscope (Olympus BX-51) and a stereology software package (Stereo Investigator v7.5) were used to apply the optical fractionator method (Gundersen et al. 1988) for estimating GFP-containing and double-labeled structures. Eight sections were determined (systematic, uniformly random sampling) for evaluation to obtain an acceptable counting precision where the coefficient of error (CE) is smaller than 5% by applying an unbiased counting frame covering an area of 10,000 μm^2 (Slomianka and West 2005). The optical disector (West et al. 1991) volume of tissue was 25,000 μm^3 (40× objective). After counting GFP and GFP-nestin double-labeled structures in 110 counting frames on average, we normalized counts to mm^3 (numerical density) and calculated ratios (%) of doubled labeled to only GFP-labeled cells.

To estimate the total number of cells infected by viruses the region containing these cells need to be identified unambiguous. However, due to stereotactic injection,

diffusion processes of the injected viruses, interindividual variability, survival time and age of animals the spatial distribution of infected cells turned out be inhomogeneous with a maximum around the injection canal. Furthermore, some infected cells can be encountered also at the dorsal part of the DG. Hence, the spatial delineation of those parts of the hippocampus where viruses infected cells (GFP-expression) located between a first and last tissue slide containing GFP-expressing cells gives rise to a relative large source of variability of identification. However, we aimed to know the number of infected cells in a representative region of interest, respectively, volume in the injection area. Therefore, volume densities of normalized regions containing infected cells were calculated.

Statistical testing of mean density values of the three time points was done with SPSS (v15.0.1) using the nonparametric *U* test. The minimum level of statistical significance was set at $p < 0.05$. The estimated densities are expressed as mean ± SEM. For documentation of various stainings mounted tissue slices were analyzed and documented with a Leitz Aristoplan microscope (Wetzlar, Germany) equipped with the appropriate fluorescence filter units for GFP-, AMCA- and Cy3-detection and images were generated with a digital camera (Diagnostic Instruments, Sterling Heights, MI, USA). Documentation was also performed with a confocal laser scanning microscope (Nikon Eclipse E400 with the confocal system C1).

Results

We have previously shown that the peptide-tagged Ad vector AdGFPL.VPTQSSG mediates specific gene delivery to hippocampal stem cells after direct virus injection into the mouse brain (Schmidt et al. 2007). The selective transduction of target cells by AdGFPL.VPTQSSG in the adult rat hippocampus was demonstrated by GFP expression of cells laying in the dentate gyrus (DG, Fig. 1a–c). Since the natural tropism of this virus via the Coxsackie-Adenovirus-Receptor (CAR) is completely depleted, binding and internalization into target cells occur exclusively through the covalently linked peptide (Schmidt et al. 2007). GFP-labeling was restricted to the DG (Fig. 1b) where mainly the radial glia-like type-1 cells expressed GFP (Fig. 1c). The injection of peptide-tagged Ad vector in the SVZ (Fig. 1d), the second stem cell homing region in the adult brain, did not result in an efficient and specific transduction of cells. Only few single cells with the morphology of astrocytes expressed the marker protein GFP (Fig. 1e).

Three days after direct administration of Ad vector into the DG, brain sections stained for GFAP (blue, Fig. 2a2) and NeuN (red, Fig. 2a3) showed GFP-containing type-1 cell somata located in the subgranular zone that are GFAP positive (Fig. 2a4). At this time point, transduced cells did not express the neuronal cell marker NeuN. In contrast, counterstaining of brain slices revealed a marked increase of NeuN or GFAP expressing cells that were also GFP-positive at day 30 (Fig. 2b–b3), whereas 90 days post-injection only type-1 cells or mainly astrocytes contained GFP (Fig. 2c–c3).

To further characterize transduced cells by stem cell markers, parallel serial sections were incubated with antibodies directed against nestin and tissue slices were also documented by confocal laser scanning microscopy (Fig. 3). Three days after Ad vector injection, we found a general increase of nestin-positive cells in the hilar region of the hippocampus, mainly in direct vicinity of the Ad vector injection site (Fig. 3a). This has not been observed in the contralateral, non-injected side (not shown). A strong co-localization of GFP-transduced cells with nestin was clearly detectable and the radial glia-like morphology of cells was obvious (Fig. 3a1–a3), whereas after 30 (Fig. 3b–b3) and 90 days (Fig. 3c–c3) the amount of GFP-expressing stem cells gradually decreased. However, 30 days after virus injection, GFP-containing cells with the morphology of mature (Fig. 3b) or young neurons (Fig. 3b1–b3) that did not contain nestin appeared. After 90 days, the majority of GFP-positive cells exhibited glial cell type specific features (Fig. 3c).

Unbiased stereologic counting of transduced cells in the DG was performed to estimate the number of initially transduced NSC and to follow up the changes in cell numbers over time for up to 90 days (Fig. 4). The density of GFP structures of the 3 days group was 24,067 ± 2,222.7/mm^3, for the 30 days group 14,730 ± 1.484/mm^3, and for the 90 days group 10,154.8 ± 422.8/mm^3 (Fig. 4a). In comparison, the numerical density for double-labeled GFP-nestin containing cells was 19,861 ± 2,032.9/mm^3 (3 days group), 8,108.2 ± 642.9/mm^3 (30 days group), and 2,875.8 ± 464.6/mm^3 (90 days group) (Fig. 4b). As shown in Fig. 4c, the mean fraction of GFP-expressing nestin-positive cells in the group of 3 days was 82.3 ± 2.1%. After 30 days this relation decreased to 56.3 ± 3.2% ($p = 0.016$). After 90 days of injection 23.4 ± 4.5% double-labeled cells were found ($p = 0.06$). These data indicate that a proportion of Ad vector infected stem cells maturates to neurons within 4 weeks of infection (Fig. 2b–b3, 3b–b3). Between 30 and 90 days these neurons disappear and after 3 months only GFP-expressing type-1 cells or astrocytes were found.

Discussion

In the present study, we demonstrate that a CAR-ablated Ad vector coupled to the VPTQSSG peptide mediates

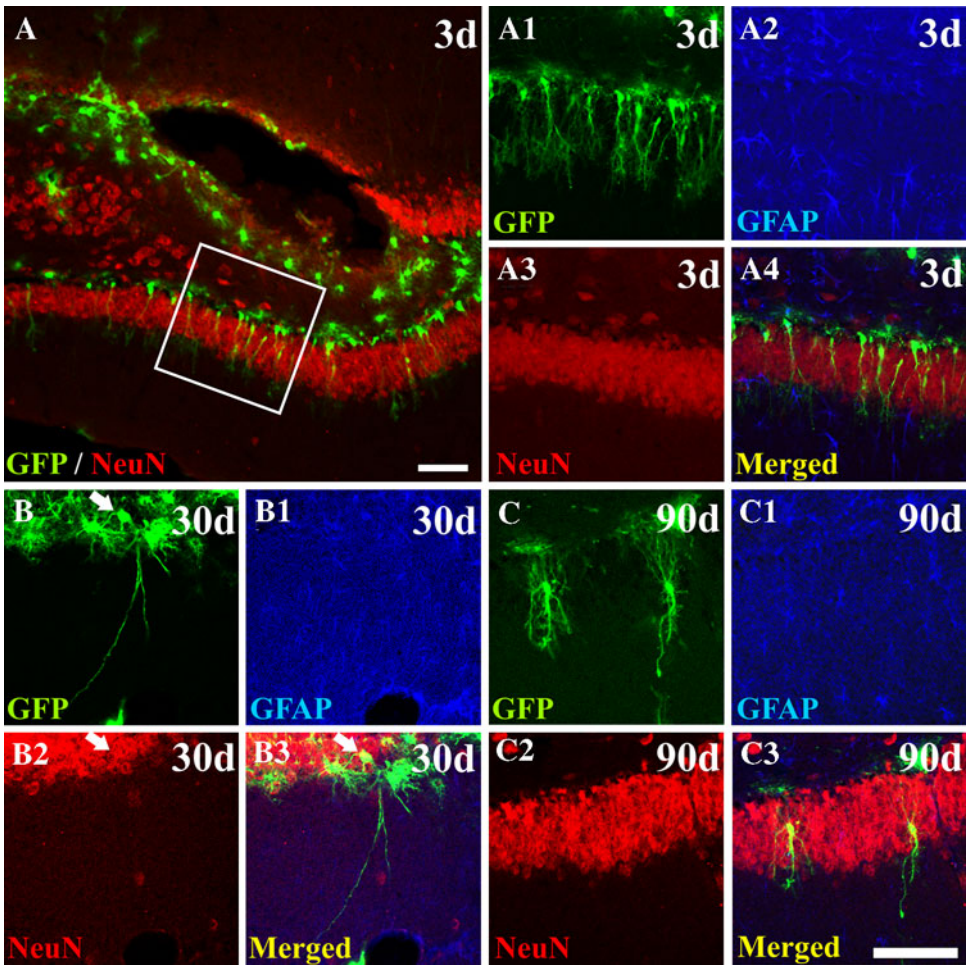

Fig. 2 Differentiation patterns of transduced cells as revealed by confocal laser scanning microscopy. **a** Overview of a section at day 3 after virus injection in direct vicinity of the injection site counterstained for NeuN (*red fluorescence*). In the DG numerous GFP-expressing type-1 cells with a subgranular soma possessing a single process penetrating the granular layer were observed. The frame (**a**) points out the region of higher magnifications containing mainly GFP-expressing type-1 cells (*green* **a1**) counterstained for GFAP (blue, **a2**) and NeuN (*red* **a3**). In higher magnification, the co-localization of GFP and GFAP was demonstrated; GFP-expressing cells never contained NeuN (**a4**). **b** After 30 days, single GFP-expressing neurons with their soma in the granule cell layer (*arrow*) and dendrites in the molecular layer were observed. In triple labeling of such a region for GFAP (**b1**) and NeuN (**b2**) the NeuN-GFP coexpression is shown (**b3**). c After 90 days of survival, only GFP-expressing astrocytes or type-1 cells (not shown here), were found in the DG (labeling as in **b**). *Scale bars* 100 µm

efficient transduction of stem cells in the adult rat hippocampus in a highly specific manner. Our aim was to show that the peptide identified from murine hippocampus has the same specificity for NSC in the rat hippocampus. Regarding infection of NSC from the subventricular zone (SVZ), another stem cell homing region, we observed similar results in the rat as compared to the mouse brain where NSC of this region were not transduced by the modified viruses (Schmidt et al. 2007). In situ infection was restricted to NSC of the CNS region where they were isolated from, suggesting that intrinsic differences in NSC between hippocampus and SVZ also exist in the adult rat brain. Strikingly, by this labeling method the pool of slowly dividing NSC seemed to be distributed more prominently in the DG compared to type-2 cells. It has been shown that these type-1 or radial glia cells in the adult DG (Seki and Arai 1999; Shapiro et al. 2005) are able to self-renew, to contribute to neuronal migration and to generate—in addition to astrocytes—neurons (Shapiro et al. 2005; Seri et al. 2001; Alvarez-Buylla et al. 2002; Gubert et al. 2009). Compared to the classical indication methods by labeling the rapidly dividing type-2 cells in the adult hippocampus (Altman and Das 1965; Dolbeare 1995; Kronenberg et al. 2003; Geraerts et al. 2006; Kempermann 2006; Zhao et al. 2006; Ge et al. 2007), we could stain directly the population of slowly dividing type-1 cells. The stem cell character of GFP-expressing cells was confirmed by their radial glia-like morphology, and by co-labeling

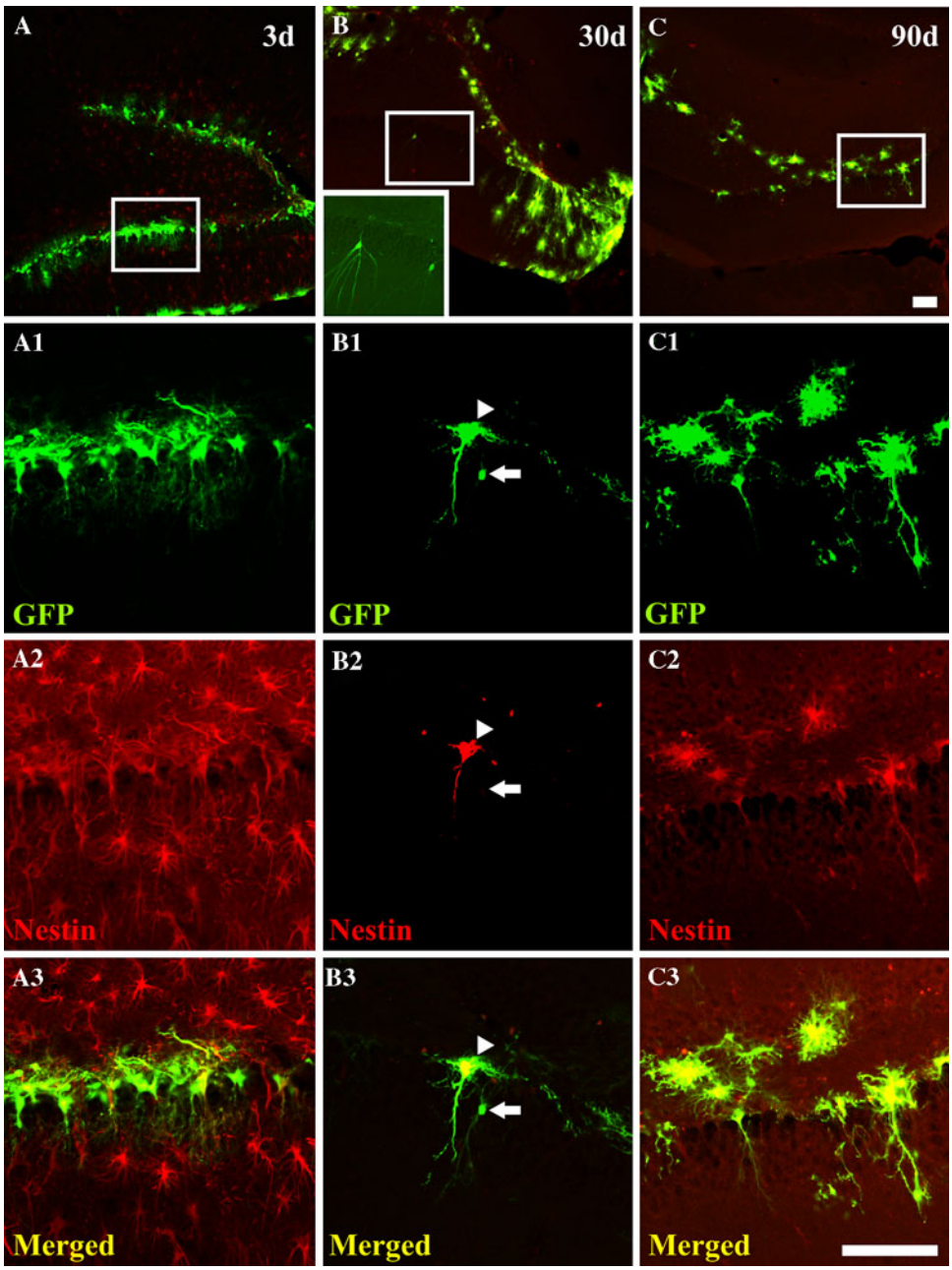

Fig. 3 Overview of long-term GFP-expressing cells counterstained for nestin demonstrated by confocal laser scanning microscopy. **a** Overview of a section containing numerous transduced cells (*green*), 3 days after virus injection. The frame depicts the region of higher magnifications (**a1–a3**). The type-1 cell morphology (**a1**) and their co-expression with nestin (*red* **a2**) was demonstrated by merging (**a3**, *yellow*). **b** Thirty days after injection, the decrease of GFP and nestin-containing cells is obvious. At this time point, single GFP containing neurons (frame and in higher magnification in the *inset*) were detectable. Thirty days after virus injection, GFP-labeled type-1 cells (**b1**) that express nestin (**b2** *arrowhead*), but now also other GFP-containing nestin-negative cells (**b2**, *arrow*) with the morphology of immature neurons can be detected (merge **b3**). **c** Long-term expression of GFP in nestin-containing cells can be observed at least 90 days post-injection. At this time point, no GFP-expressing neurons were detectable. The frame depicts the region of higher magnifications (**c1**). GFP-containing (*green*) astrocytes and also type-1 cells with their radial glia-like morphology were immunoreactive for nestin (*red* **c2**) as demonstrated by merging (*yellow* **c3**). *Scale bars* **a–c** 150 μm, **a1–a3**, **b1–b3**, **c1–c3** 100 μm

with nestin or GFAP (Malatesta et al. 2003; Anthony et al. 2004). The broad distribution of the intermediate protein nestin has been examined in the adult brain (Dahlstrand et al. 1992, 1995), where nestin was found not only in stem, but also in progenitor and differentiated cells. In our experiments, we observed an upregulation of nestin also in astrocytes of the hippocampal hilar region. This is well known from manipulated conditions in the brain and most likely due to a small injury during virus injection, indicating that these nestin-like immunoreactive cells belong to a reactive population of astrocytes and not to NSC (Duggal et al. 1997; Chen et al. 2002; Yoo et al. 2005). In our approach, we used the advantages of stereological techniques to determine relatively unbiased estimates of marker gene-expressing cells and of NSC after labeling of nestin in the DG as well as double-labeled cells. The number of GFP-positive cells in the granule cell layer declined between day 3 and 90 days after infection resulting in ~2.7 and 0.9% labeled cells at day 30 and 90, respectively.

There could be several reasons why we observed reduced numbers of GFP and/or GFP-nestin containing cells in the DG over time. The lower cell numbers can be explained, for example, by multiple cell proliferations and therefore dilution of Ad vector. Adenovirus is not integrated into the host genome, and therefore, the amount of viral particles to

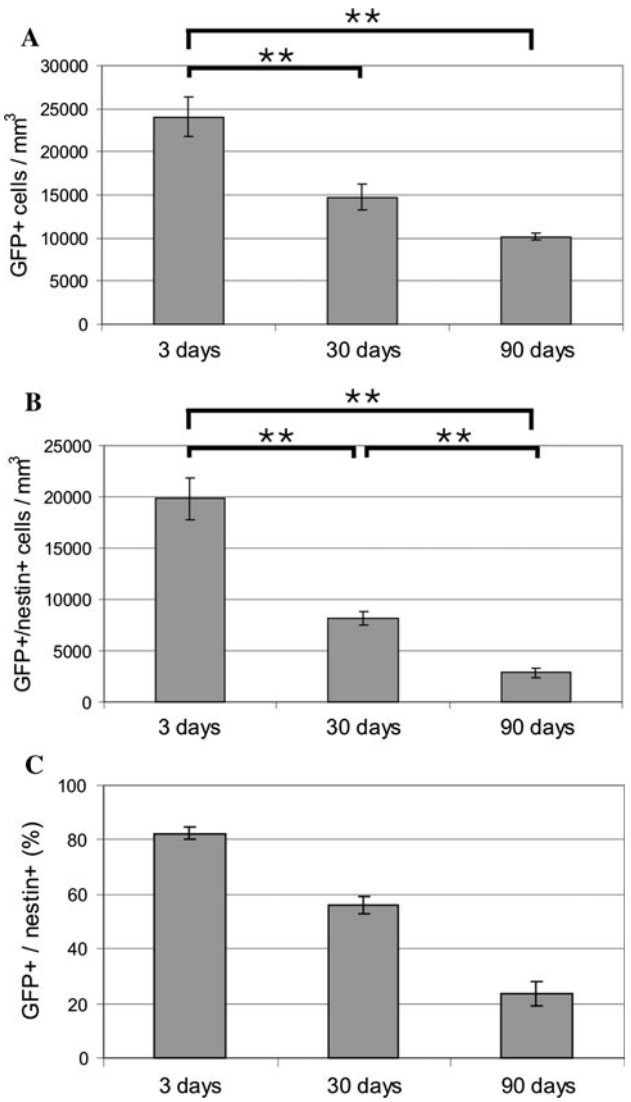

Fig. 4 Stereologic evaluation of transduced cells. **a** The density of GFP structures was 24,067 ± 2,222.7/mm^3 after 3 days (*left column*), 14,730 ± 1,484/mm^3 for 30 days (*middle column*) and 10,154.8 ± 422.8/mm^3 after 90 days (*right column*). **b** Double-labeled GFP-nestin containing cells were 19,861 ± 2,032.9/mm^3 (3 days, *left column*), 8,108.2 ± 642.9/mm^3 (30 days, *middle column*) and 2,875.8 ± 464.6/mm^3 (90 days, *right column*). **c** Presentation of GFP-nestin double-labeled cells in percent revealed the following results: 82.3 ± 2.1% GFP-expressing and nestin-containing double-labeled cells (3 days, *left*), 56.3 ± 3.2% (30 days, $p = 0.016$, *middle*) and 23.4 ± 4.5% (90 days, $p = 0.06$, *right*)

generate detectable levels of GFP is reduced from cell to cell division. Similar findings concerning the dilution of a marker in the early phase of proliferation after BrdU-labeling have also been described (Dayer et al. 2003). Another potential cause may be downregulation of the transgene, although this is rather unlikely, because previous studies have shown a relatively stable Ad vector-mediated gene expression in the central nervous system over a several months time period (Kirik et al. 2000; Thomas et al. 2001). Furthermore, neuronal properties were found only in cells 30 days after injection, but not at day 90. In our previous study (Schmidt et al. 2007) we found only a limited immune response 3 days after virus injection and longer survival were not investigated. Therefore, one possibility for the paucity of the long-term GFP-expression could be that these cells are selectively or at least preferentially eliminated. Such immunological reactions in the brain can occur after Ad vector injection (Thomas et al. 2001). We did not detect pyknotic or dying GFP-containing cells 3 months post-injection. Unfortunately, we not investigate time points between 30 and 90 days and therefore cannot present results or hints concerning the decrease in number of GFP-containing nerve cells. However, at 30 days post-injection the number of GFP-containing cells possessing granular nerve cell morphology or GFP/NeuN-containing cells was very low. We only detected about 10–12 of those cells per animal and therefore stereological cell number estimation was not performed. These numbers are very low compared to long-time studies in rats performed by Dayer et al. (2003). They showed that 6 months after a single BrdU-injection the whole bilateral dentate gyrus contained about 5,000 BrdU-immunoreactive cells and that more than 86% of them were also NeuN-immunoreactive. However, the results of our stereotactic labeling paradigm and the systemic application of BrdU cannot be compared because Ad-vector dilution is restricted to a certain area in the injected hemisphere and not to the whole bilateral hippocampus. However, the apparent loss of particularly NeuN-positive cells in our study is in line with data from Kempermann et al. (1998), who showed that BrdU-positive cells decrease by approximately 60% per month after labeling. Extrapolating this rate of loss, one would expect about 6% of BrdU-positive cells to be present after 12 weeks. Considering these data (285 NeuN-/BrdU-positive cells after 4 weeks in control mice), this results in 45 NeuN-positive cells in the entire DG, which lowers the probability of finding one NeuN-positive cell per slice to <0.5. Assuming that cell death particularly affects neuronal cell types, this probability might be even substantially lower (Biebl et al. 2000).

Another advantage of this selective method for NSC labeling is that mainly the slow dividing type-1 cell population (Kempermann et al. 2004) can be tagged and that at least during short time differentiation processes the GFP expression allows tracking of infected cells, respectively, their daughter cells. The presented labeling method in the rat brain can now be applied to a variety of experimental approaches such as investigations of influence of the surrounding microenvironment on the number of NSC, neurogenesis and the maturation of neurons in adult rodent brains (van Praag et al. 2000) or electrophysiological development of neurons derived from NSC (Schmidt-Hieber et al. 2004).

In summary we provide evidence that Ad vectors modified to target adult hippocampal stem cells in mice can also be used in rats. This finding is of particular interest because it clearly demonstrates that the as yet unknown receptor on the surface of the NSCs is not species specific. This knowledge broadens the number of animal models that can be used to monitor stem cell development and migration, and has great implications for studying their impact on CNS disorders or therapeutic potential against them.

Acknowledgments We thank Frauke Winzer and Susann Lehmann for skillful technical assistance. We are grateful to Ramon Alemany for providing AdTLY477RAE vector. Grant sponsor: Bundesminister für Bildung und Forschung (to B.M.P.); Grant number: 01ZZ0108; Grant sponsor: Deutsche Forschungsgemeinschaft (to B.M.P. and A.W.); Grant numbers: PU188/8-1 and WR20/2-1; Grant sponsor: FORUN program Medical Faculty of Rostock (to A.S. and S.J.-P.H); Grant numbers: 889048 and 889011.

References

Alemany R, Curiel DT (2001) CAR-binding ablation does not change biodistribution and toxicity of adenoviral vectors. Gene Ther 8:1347–1353

Altman J, Das GD (1965) Autoradiographic and histological evidence of postnatal hippocampal neurogenesis in rats. J Comp Neurol 124:319–335

Alvarez-Buylla A, Seri B, Doetsch F (2002) Identification of neural stem cells in the adult vertebrate brain. Brain Res Bull 57:751–758

Anthony TE, Klein C, Fishell G, Heintz N (2004) Radial glia serve as neuronal progenitors in all regions of the central nervous system. Neuron 41:881–890

Biebl M, Cooper CM, Winkler J, Kuhn HG (2000) Analysis of neurogenesis and programmed cell death reveals a self-renewing capacity in the adult rat brain. Neurosci Lett 291:17–20

Chen LW, Wei LC, Qiu Y, Liu HL, Rao ZR, Ju G, Chan YS (2002) Significant up-regulation of nestin protein in the neostriatum of MPTP-treated mice. Are the striatal astrocytes regionally activated after systemic MPTP administration? Brain Res 925:9–17

Curtis MA, Penney EB, Pearson AG, Van Roon-Mom WM, Butterworth NJ, Dragunow M, Connor B, Faull RL (2003) Increased cell proliferation and neurogenesis in the adult human Huntington's disease brain. Proc Natl Acad Sci USA 100: 9023–9027

Dahlstrand J, Zimmerman LB, Mckay RD, Lendahl U (1992) Characterization of the human nestin gene reveals a close evolutionary relationship to neurofilaments. J Cell Sci 103:589–597

Dahlstrand J, Lardelli M, Lendahl U (1995) Nestin mRNA expression correlates with the central nervous system progenitor cell state in many, but not all, regions of developing central nervous system. Brain Res Dev Brain Res 84:109–129

Dayer AG, Ford AA, Cleaver KM, Yassaee M, Cameron HA (2003) Short-term and long-term survival of new neurons in the rat dentate gyrus. J Comp Neurol 460:563–572

Dolbeare F (1995) Bromodeoxyuridine: a diagnostic tool in biology and medicine, part II: oncology, chemotherapy and carcinogenesis. Histochem J 27:923–964

Duggal N, Schmidt-Kastner R, Hakim AM (1997) Nestin expression in reactive astrocytes following focal cerebral ischemia in rats. Brain Res 768:1–9

Eriksson PS, Perfilieva E, Bjork-Eriksson T, Alborn AM, Nordborg C, Peterson DA, Gage FH (1998) Neurogenesis in the adult human hippocampus. Nat Med 4:1313–1317

Ge S, Yang CH, Hsu KS, Ming GL, Song H (2007) A critical period for enhanced synaptic plasticity in newly generated neurons of the adult brain. Neuron 54:559–566

Geraerts M, Eggermont K, Hernandez-Acosta P, Garcia-Verdugo JM, Baekelandt V, Debyser Z (2006) Lentiviral vectors mediate efficient and stable gene transfer in adult neural stem cells in vivo. Hum Gene Ther 17:635–650

Graham FL, Prevec L (1995) Methods for construction of adenovirus vectors. Mol Biotechnol 3:207–220

Gubert F, Zaverucha-Do-Valle C, Pimentel-Coelho PM, Mendez-Otero R, Santiago MF (2009) Radial glia-like cells persist in the adult rat brain. Brain Res 1258:43–52

Gundersen HJ, Bagger P, Bendtsen TF, Evans SM, Korbo L, Marcussen N, Moller A, Nielsen K, Nyengaard JR, Pakkenberg B (1988) The new stereological tools: disector, fractionator, nucleator and point sampled intercepts and their use in pathological research and diagnosis. Apmis 96:857–881

Kempermann G (2006) Adult neurogenesis: stem cells and neuronal development in the adult brain. Oxford University Press, New York

Kempermann G, Kuhn HG, Gage FH (1998) Experience-induced neurogenesis in the senescent dentate gyrus. J Neurosci 18:3206–3212

Kempermann G, Jessberger S, Steiner B, Kronenberg G (2004) Milestones of neuronal development in the adult hippocampus. Trends Neurosci 27:447–452

Kirik D, Rosenblad C, Björklund A, Mandel RJ (2000) Long-term, rAAV-mediated gene transfer of GDNF in the rat Parkinson's model: intrastriatal but not intranigral transduction promotes functional regeneration in the lesioned nigrostriatal system. J Neurosci 20:4686–4700

Kronenberg G, Reuter K, Steiner B, Brandt MD, Jessberger S, Yamaguchi M, Kempermann G (2003) Subpopulations of proliferating cells of the adult hippocampus respond differently to physiologic neurogenic stimuli. J Comp Neurol 467:455–463

Malatesta P, Hack MA, Hartfuss E, Kettenmann H, Klinkert W, Kirchhoff F, Gotz M (2003) Neuronal or glial progeny: regional differences in radial glia fate. Neuron 37:751–764

Ming GL, Song H (2005) Adult neurogenesis in the mammalian central nervous system. Annu Rev Neurosci 28:223–250

O'Riordan CR, Lachapelle A, Delgado C, Parkes V, Wadsworth SC, Smith AE, Francis GE (1999) PEGylation of adenovirus with retention of infectivity and protection from neutralizing antibody in vitro and in vivo. Hum Gene Ther 10:1349–1358

Overstreet LS, Hentges ST, Bumaschny VF, de Souza FSJ, Smart JL, Santangelo AM, Low MJ, Westbrook GL, Rubinstein M (2004) A transgenic marker for newly born granule cells in dentate gyrus. J Neurosci 23:3251–3259

Paxinos G (1986) The rat brain in stereotaxic coordinates, 2nd edn. Academic Press, London

Pützer BM, Gnauck J, Kirch HC, Brockmann D, Esche H (1997) A cis-acting element 7 bp upstream of the ESF-1-binding motif is involved in E1A 13S autoregulation of the adenovirus 12 TS2 promoter. J Gen Virol 78:879–891

Pützer BM, Stiewe T, Parssanedjad K, Rega S, Esche H (2000) E1A is sufficient by itself to induce apoptosis independent of p53 and other adenoviral gene products. Cell Death Differ 7:177–188

Romanczuk H, Galer CE, Zabner J, Barsomian G, Wadsworth SC, O'Riordan CR (1999) Modification of an adenoviral vector with

biologically selected peptides: a novel strategy for gene delivery to cells of choice. Hum Gene Ther 10:2615–2626

Schmidt A, Haas SJ, Hildebrandt S, Scheibe J, Eckhoff B, Racek T, Kempermann G, Wree A, Pützer BM (2007) Selective targeting of adenoviral vectors to neural precursor cells in the hippocampus of adult mice: new prospects for in situ gene therapy. Stem Cells 25:2910–2918

Schmidt-Hieber C, Jonas P, Bischofberger J (2004) Enhanced synaptic plasticity in newly generated granule cells of the adult hippocampus. Nature 429:184–187

Schmitt O, Eggers R (1997) Systematic investigations of the contrast results of histochemical stainings of neurons and glial cells in the human brain by means of image analysis. Micron 28:197–215

Seki T, Arai Y (1999) Temporal and spacial relationships between PSA-NCAM-expressing, newly generated granule cells, and radial glia-like cells in the adult dentate gyrus. J Comp Neurol 410:503–513

Seri B, Garcia-Verdugo JM, Mcewen BS, Alvarez-Buylla A (2001) Astrocytes give rise to new neurons in the adult mammalian hippocampus. J Neurosci 21:7153–7160

Shapiro LA, Korn MJ, Shan Z, Ribak CE (2005) GFAP-expressing radial glia-like cell bodies are involved in a one-to-one relationship with doublecortin-immunolabeled newborn neurons in the adult dentate gyrus. Brain Res 1040:81–91

Slomianka L, West MJ (2005) Estimators of the precision of stereological estimates: an example based on the CA1 pyramidal cell layer of rats. Neuroscience 136:757–767

Song H, Kempermann G, Overstreet Wadiche L, Zhao C, Schinder AF, Bischofberger J (2005) New neurons in the adult mammalian brain: synaptogenesis and functional integration. J Neurosci 25:10366–10368

Steiner B, Klempin F, Wang L, Kott M, Kettenmann H, Kempermann G (2006) Type-2 cells as link between glial and neuronal lineage in adult hippocampal neurogenesis. Glia 54:805–814

Thomas CE, Abordo-Abesida E, Maleniak TC, Stone D, Gerdes CA, Lowenstein PR (2001) Gene transfer into rat brain using adenoviral vectors. Curr Prot Neurosci Chapter 4:Unit 4.24

van Praag H, Kempermann G, Gage FH (2000) Neural consequences of environmental enrichment. Nat Rev Neurosci 1:191–198

van Praag H, Schinder AF, Christie BR, Toni N, Palmer TD, Gage FH (2002) Functional neurogenesis in the adult hippocampus. Nature 415:1030–1034

West MJ (1993) New stereological methods for counting neurons. Neurobiol Aging 14:275–285

West MJ, Slomianka L, Gundersen HJ (1991) Unbiased stereological estimation of the total number of neurons in the subdivisions of the rat hippocampus using the optical fractionator. Anat Rec 231:482–497

Yoo YM, Lee U, Kim YJ (2005) Apoptosis and nestin expression in the cortex and cultured astrocytes following 6-OHDA administration. Neurosci Lett 382:88–92

Zhao C, Teng EM, Summers RG Jr, Ming GL, Gage FH (2006) Distinct morphological stages of dentate granule neuron maturation in the adult mouse hippocampus. J Neurosci 26:3–11